Journal of Medicinal Chemistry

ARTICLE

pubs.acs.org/jmc

Theonellasterols and Conicasterols from *Theonella swinhoei*. Novel Marine Natural Ligands for Human Nuclear Receptors

Simona De Marino,[†] Raffaella Ummarino,[†] Maria Valeria D'Auria,[†] Maria Giovanna Chini,[‡] Giuseppe Bifulco,[‡] Barbara Renga,[§] Claudio D'Amore,[§] Stefano Fiorucci,[§,⊥] Cécile Debitus,[∥] and Angela Zampella*[,†,⊥]

[†]Dipartimento di Chimica delle Sostanze Naturali, Università di Napoli "Federico II", via D. Montesano 49, 80131 Napoli, Italy

[‡]Dipartimento di Scienze Farmaceutiche, Università di Salerno, via Ponte don Melillo, 84084 Fisciano (SA), Italy

[§]Dipartimento di Medicina Clinica e Sperimentale, Università di Perugia, Nuova Facoltà di Medicina e Chirurgia, Via Gerardo Dottori 1, S. Andrea delle Fratte, 06132 Perugia, Italy

[∥]Institut de Recherche pour le Développement (IRD), Polynesian Research Center on Island Biodiversity, BP529, 98713 Papeete, Tahiti, French Polynesia

Supporting Information

ABSTRACT: Silica gel column chromatography, followed by HPLC purification on the apolar fraction of the methanol extract of marine sponge *Theonella swinhoei*, resulted in the isolation of a library of 10 polyhydroxylated steroids which we named theonellasterols B−H (**1**−**7**) and conicasterols B-D (**8**−**10**). The structures were determined on the basis of extensive spectroscopic data (MS, ^{1}H and ^{13}C NMR, COSY, HSQC, HMBC, and ROESY) analysis, and the putative binding mode to nuclear receptors (NRs) has been obtained through docking calculations. Pharmacological and structure−activity relationship analysis demonstrate that these natural polyhydroxylated steroids are potent ligands of human nuclear pregnane receptor (PXR) and modulator of farnesoid-X-receptor (FXR). In addition, the molecular characterization of theonellasterol G allowed the identification of the first FXR modulator and PXR ligand so far identified. Exposure of liver cells to this agent resulted in potent induction of PXR-regulated genes and modulation of FXR-regulated genes, highlighting its pharmacological potential in the treatment of liver disorders.

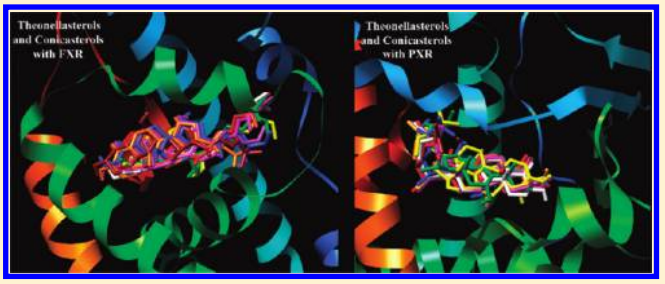

INTRODUCTION

Steroids bearing a 4-methylene group are relatively rare metabolites. They were exclusively isolated from sponges of the genus *Theonella*, mainly from *T. swinhoei,* and were unaccompanied by conventional steroids and are proposed as ideal taxonomic markers for sponges of the genus *Theonella*.[1] Since the isolation, by Djerassi et al., of conicasterol and theonellasterol (Figure 1) from *T. conica* and *T. swinhoei*,[2] respectively, about 20 new 4-methylene-steroids were isolated from *Theonella* sponges.[1,3−6] Common structural features are a 24-methyl and/or 24-ethyl side chain, the presence of oxygenated functions at C(3), C(7), or C(15), and of a $\Delta^{8,14}$ double bond rarely replaced by a 8(14)-seco-skeleton.

As a part of our systematic study on the chemical diversity and bioactivity of secondary metabolites from marine organisms collected at Solomon Islands,[7] we found a single specimen of the sponge *Theonella swinhoei* as an extraordinary source of new metabolites. Analysis of the polar extracts afforded anti-inflammatory perthamides C−D,[8,9] solomonamides A−B,[10] and solomonsterols A−B.[11]

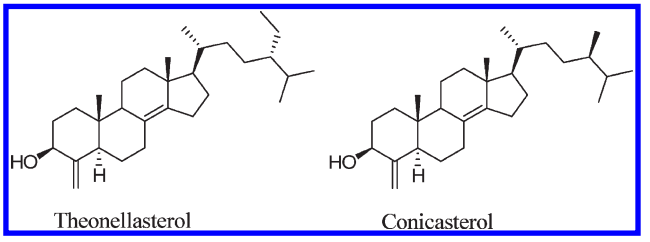

Figure 1. Theonellasterol and conicasterol previously isolated from *Theonella* species.

In the present study, we report the results of the chemical analysis of the less polar extracts, which resulted in the isolation and identification of theonellasterol[2] together with 10 new polyoxygenated steroids, which we named theonellasterols B−H (**1**−**7**) and conicasterols B-D (**8**−**10**) (Figures 2 and 3).

Received: February 16, 2011
Published: March 24, 2011

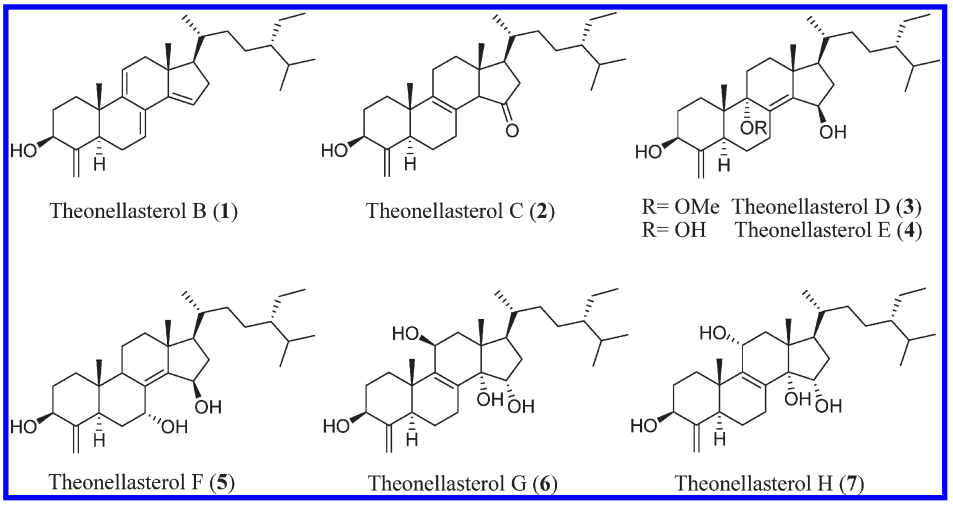

Figure 2. Theonellasterols from *Theonella swinhoei*.

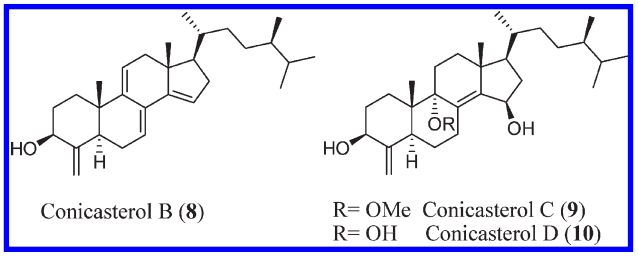

Figure 3. Conicasterols from *Theonella swinhoei*.

These marine steroids are endowed with potent agonistic activity on the human pregnane-X-receptor (PXR) while antagonize the effect of natural ligands for the human farnesoid-X-receptor (FXR). Exploiting these properties, we have identified theonellasterol G (**6**) as the first example of PXR agonist and FXR modulator from marine origin that might have utility in treating liver disorders.

RESULTS AND DISCUSSION

Chemistry. Theonellasterol B (**1**) was isolated as pale-yellow oil. The molecular formula of $C_{30}H_{46}O$ was established by HR ESIMS based on the pseudomolecular ion $[M + Li]^+$ at m/z 429.3729 (calculated 429.3709), indicating eight degrees of unsaturation. The ^{1}H NMR spectrum of **1** (Table 2 and Table S1 in Supporting Information, C_6D_6)[12] showed signals characteristic of a 4-methylene-24-ethyl steroidal system: two methyl singlets (δ_H 0.89 and 0.98), three methyl doublets (δ_H 0.90, 0.92 and 1.01), one methyl triplet (δ_H 0.95), two broad singlets at δ_H 4.77 and 5.33, and one methine proton on an oxygenated carbon at δ_H 3.67. The low-field portion of the ^{1}H NMR spectrum also contained signals relative to three olefinic protons at δ_H 6.10 (1H, br d, J = 5.6 Hz, H-7), δ_H 5.85 (1H, br s, H-15) and δ_H 5.50 (1H, br d, J = 6.5 Hz, H-11).

The ^{13}C NMR (Table 1 and Table S1 in Supporting Information) interpreted with the help of the HSQC experiment, evidenced a C30 steroidal theonellasterol skeleton with three cross-conjugated trisubstituted double bonds [UV (MeOH): λ_{max} (log ε) 275 nm (3.62)]. The localization of the double bonds follows from the analysis of COSY and HMBC data (Table S1 in Supporting Information).

In particular, COSY correlations delineated the spin system H-1 through H-7, which included one hydroxyl group at C3, the exocyclic double bond at C4, and a double bond at C7 position. The olefinic proton H-7 at δ_H 6.10 showed a long-range coupling with H-11 at δ_H 5.50 that was consistent with a double bond at the C9/C11 position, further supported by HMBC cross-peaks from Me-19 to C9 and from H-11 to C10. Finally, the last trisubstituted double bond was placed at C14/C15 on the basis of diagnostic HMBC cross-peak from Me-18 to C14. The configuration at C24 was determined by comparison of ^{13}C NMR data (Table 1) with the epimeric steroidal side chain.[13,14]

Therefore, theonellasterol B (**1**) was elucidated as 4-methylene-24(*S*)-ethylcholest-7,9(11),14-trien-3β-ol.

The molecular formula of theonellasterol C (**2**) was determined to be $C_{30}H_{48}O_2$ by HR ESIMS with $[M + Li]^+$ at m/z 447.3834 (calcd 447.3814), possessing seven degrees of unsaturation. Analysis of 2D NMR spectra clearly evidenced the same A ring and C24-ethyl side chain as in **1** (Table S2 in Supporting Information). ^{13}C NMR data (Table 1) indicated the presence of a tetrasubstituted double bond (δ_C 122.5, s and 138.6, s) and one carbonyl (δ_C 214.8). Proton signals due to H_2-7 (δ_H 2.15 and 2.51), H_2-11 (δ_H 1.82 and 2.04), and H-14 (δ_H 2.30) showed chemical shifts consistent with allylic hydrogens and a double bond at the C8/C9 position that was further supported by an HMBC cross-peak from Me-19 to C-9. The carbonyl group was placed at C15 on the basis of ^{13}C chemical shifts of C14 and C16 and of diagnostic HMBC correlations from H_2-16 and H-14 to C15.

Hence, the structure of theonellasterol C (**2**) was determined as 3β-hydroxy-4-methylene-24(*S*)-ethylcholest-8(9)-en-15-one.

The molecular formula of theonellasterol D (**3**), $C_{31}H_{52}O_3$, indicated one carbon more than a conventional theonellasterol-like skeleton. ^{1}H and ^{13}C NMR data (Tables 1−2 and Table S3 in Supporting Information) evidenced a methoxy group (δ_H 3.07, δ_C 51.1), one tetrasubstituted double bond (δ_C 132.2, s and 153.7, s), and one secondary hydroxyl group (δ_H 4.60, δ_C 70.0). The tetrasubstituted double bond was placed at 8(14) position on the basis of diagnostic HMBC correlation (Figure 4) from Me-18 to C14 and confirmed by the long-range correlations H-15 and H_2-7 to C8 and C14. Analogously, the HMBC correlations Me-19/C9 and OMe/C9 support the localization

Table 1. ^{13}C NMR Data for Compounds 1−10 (175 and 125 MHz, C_6D_6)

	compd									
C	1	2	3	4	5	6	7	8	9	10
1	35.4	34.9	29.6	30.1	36.9	34.3	34.6	35.4	29.5	30.0
2	33.4	32.9	33.3	33.3	33.5	32.9	33.0	33.3	33.3	33.4
3	73.0	72.9	73.2	73.1	73.2	72.9	72.8	73.1	73.1	73.1
4	154.0	152.9	154.3	154.2	153.4	152.4	152.7	154.2	154.3	154.1
5	43.9	46.9	41.6	41.7	43.2	46.4	46.2	44.0	41.6	41.7
6	26.3	21.3	25.3	24.8	31.6	20.8	20.7	26.2	25.3	24.7
7	121.1	29.9	27.2	27.1	66.7	25.9	26.9	121.1	27.2	27.2
8	128.4	122.5	132.2	135.4	136.7	133.6	138.4	128.3	132.1	135.3
9	142.5	138.6	77.8	74.5	45.6	142.5	141.4	142.7	77.8	74.5
10	38.5	40.1	45.0	43.7	40.0	37.6	38.7	38.3	45.0	43.8
11	118.6	21.9	26.5	29.2	20.3	71.2	64.9	118.6	26.5	29.1
12	42.7	32.3	37.5	34.5	38.1	39.9	45.0	42.7	37.4	34.4
13	45.6	41.0	43.6	44.2	43.8	45.0	49.8	45.5	43.4	44.2
14	148.3	65.7	153.7	150.2	151.5	89.7	83.7	148.3	153.7	150.3
15	118.0	214.8	70.0	69.8	70.2	71.3	71.6	118.1	70.0	69.8
16	36.2	40.7	39.4	39.4	39.5	40.0	39.6	36.2	39.4	39.4
17	58.6	42.6	54.3	53.7	53.5	51.8	52.0	58.4	54.2	53.7
18	18.0	22.6	18.1	18.2	19.9	20.6	19.9	18.0	18.1	18.3
19	19.8	18.3	17.1	16.9	12.9	18.6	18.0	19.8	17.1	17.0
20	35.0	35.4	34.6	34.5	34.6	36.9	36.9	34.9	35.0	34.9
21	19.2	19.3	19.3	19.5	19.4	18.8	18.6	19.3	19.1	19.2
22	34.3	33.7	34.2	34.3	34.2	34.1	34.1	33.8	33.8	33.8
23	26.7	27.5	26.8	26.7	26.8	27.4	27.3	30.6	30.6	30.6
24	46.6	46.3	46.6	46.6	46.7	46.6	46.5	39.2	39.2	39.2
25	29.3	29.3	29.2	29.4	29.5	29.6	29.3	32.7	32.7	32.7
26	19.3	19.3	19.3	19.3	19.3	19.4	19.2	18.3	18.5	18.4
27	19.7	19.7	19.7	19.8	19.6	20.1	19.9	20.3	20.3	20.3
28	23.5	23.4	23.5	23.5	23.5	23.6	23.4	15.5	15.5	15.6
29	12.7	12.6	12.6	12.6	12.6	12.7	12.6	104.1	103.5	103.7
30	104.1	103.3	103.7	103.8	103.3	103.4	103.3			
OMe			51.1						51.0	

of the methoxy group at C9, whereas the 15-hydroxy function follows from $^1H,^1H$−COSY correlations.

The ROESY correlations H-5α/H-7α and H-7α/OMe implied that the methoxy group at C9 was α-oriented, which was further supported by the syn-axial γ-effects exerted by the methoxy substituent on C1, C5, and C7 and by the downfield shift of H-5. The strong ROE effect between H-15 and H-17α (Figure 4) indicated that the hydroxy group at C15 is in a β-position, as confirmed by the chemical shifts of the nuclei of ring D.[15]

On the basis of foregoing analysis the structure of theonellasterol D (**3**) was determined as 4-methylene-9α-methoxy-24(*S*)-ethylcholest-8(14)-en-3β,15β-diol.

The molecular formula of theonellasterol E (**4**) was determined as $C_{30}H_{50}O_3$, equivalent to theonellasterol D (**3**) less CH_2. Comparison with spectral data of **3**, and chemical shift arguments (Tables 1, 2 and Table S4 in Supporting Information), and 2D NMR analysis indicated that theonellasterol E (**4**) differs from **3** for a 9α-hydroxy group replacing the 9α-methoxy group, disclosing a 4-methylene-24(*S*)-ethylcholest-8(14)-en-3β,9α,15β-triol structure for theonellasterol E (**4**).

As determined by HR ESIMS measurements, theonellasterol F (**5**) is isomeric with **4**. From 1D NMR spectra, it was possible to assign a tetrasubstituted double bond and two oxygen bearing methine groups. The same $\Delta^{8,14}$-15β-hydroxy substructure as in theonellasterols D and E was inferred from 2D NMR analysis (Table S5 in Supporting Information and Figure 4). COSY correlations delineated the spin system H-1 through H-7, and the ^{13}C chemical shift for C7 (δ_C 66.7) implied an OH substitution. The relative stereochemistry at C7 was deduced from the small vicinal coupling constant of H-7, which is consistent with an equatorial disposition for this proton, thereby placing the hydroxyl group in an axial α-orientation. This was confirmed by the relatively low field shifts of H-5 and H-9 caused by the 1,3-diaxial relationship of these protons to the hydroxy group at C7 (Table 2). Thus, theonellasterol F (**5**) was defined as 4-methylene-24(*S*)-ethylcholest-8(14)-en-3β,7α,15β-triol.

Theonellasterol G (**6**) was isolated as an optically active pale-yellow oil with a molecular formula of $C_{30}H_{50}O_4$. In addition to the signals relative to 4-methylene-3β-hydroxy structure, the ^{13}C NMR spectrum of **6** (Table 1 and Table S6 in Supporting Information) showed the presence of two quaternary sp^2 carbons (δ_C 133.6 and 142.5), two oxygen-bearing methine carbons (δ_C 71.2 and 71.3), and one oxygen-bearing quaternary carbon (δ_C 89.7). The HMBC correlation between the angular methyl

dx.doi.org/10.1021/jm200169t |J. Med. Chem. 2011, 54, 3065–3075

Table 2. Selected ^{1}H NMR Data for Compounds 1−10 (700 and 500 MHz, C_6D_6)

	compd									
H	1	2	3	4	5	6	7	8	9	10
3	3.67 m	3.71 dd (5.4, 11.0)	3.89 dd (5.3, 11.2)	3.90 m	3.79 m	3.73 dd (5.7, 11.0)	3.79 m	3.65 m	3.89 dd (5.3, 11.3)	3.89 m
5	1.95 m	1.74 m	2.89 br d (12.4)	2.78 br d (12.3)	2.42 m	1.85 m	1.78 m	1.92 m	2.89 br d (12.4)	2.73 br d (12.3)
7	6.10 br d (5.6)	2.15 dd (5.6, 18.1) 2.51 m	2.16 ddd (5.3, 8.2, 13.6) 2.52 m	2.41 m 2.53 ddd (1.8, 4.8, 14.5)	4.63 br t (2.9)	2.02 dd (5.7, 18.3) 2.61 m	2.10 dd (5.8, 18.3) 2.47 m	6.08 br d (5.6)	2.15 ddd (5.3, 8.2, 13.6) 2.51 m	2.42 m 2.55 ddd (1.8, 4.7, 14.6)
9					2.41 m					
11	5.50 br d (6.5)	1.82 m 2.04 m	1.60 m 1.75 m	1.55 m 1.81 m	1.54 m	4.39 br t (2.9)	4.07 d (7.9)	5.49 br d (6.5)	1.60 m 1.75 m	1.56 m 1.83 m
15	5.85 br s		4.60 br t (4.4)	4.50 br d (6.0)	4.58 br d (4.8)	4.47 dd (6.0, 9.6)	4.19 dd (4.9, 9.6)	5.84 br s	4.61 br t (4.3)	4.51 br d (6.0)
17	1.73 m	2.00 m	1.64 m	1.62 m	1.64 m	2.40 m	2.35 m	1.73 m	1.65 m	1.62 m
18	0.98 s	0.81 s	0.73 s	0.73 s	0.79 s	0.43 s	0.49 s	0.97 s	0.73 s	0.73 s
19	0.89 s	0.82 s	0.72 s	0.71 s	0.59 s	0.59 s	0.66 s	0.87 s	0.72 s	0.70 s
21	1.01 d (6.4)	0.94 d (6.6)	1.01 d (6.6)	1.04 d (6.5)	1.02 d (6.2)	0.88 d (6.4)	0.90 d (6.4)	0.97 d (6.4)	0.98 d (6.3)	1.01 d (6.6)
26	0.90 d (7.0)	0.84 d (6.9)	0.91 d (6.8)	0.93 d (6.9)	0.93 d (6.2)	0.91 d (6.8)	0.91 d (6.8)	0.85 d (7.0)	0.88 d (6.5)	0.89 d (6.8)
27	0.92 d (7.0)	0.87 d (6.9)	0.93 d (6.8)	0.94 d (6.9)	0.94 d (6.2)	0.94 d (6.8)	0.93 d (6.8)	0.90 d (7.0)	0.93 d (6.5)	0.93 d (6.8)
28	1.22 m 1.39 m	1.14 m 1.33 m	1.23 m 1.41 m	1.24 m 1.42 m	1.23 m 1.41 m	1.22 m 1.42 m	1.22 m 1.42 m	0.85 d (7.0)	0.88 d (6.7)	0.89 d (6.8)
29	0.95 t (7.4)	0.89 t (7.4)	0.96 t (7.4)	0.96 t (7.3)	0.96 t (7.4)	0.96 t (7.3)	0.97 t (7.4)	4.77 br s 5.33 br s	4.74 br s 5.35 br s	4.76 br s 5.36 br s
30	4.77 br s 5.33 br s	4.69 br s 5.24 br s	4.75 br s 5.36 br s	4.76 br s 5.36 br s	4.73 br s 5.33 br s	4.67 br s 5.28 br s	4.71 br s 5.30 br s			
OMe			3.07 s						3.07 s	

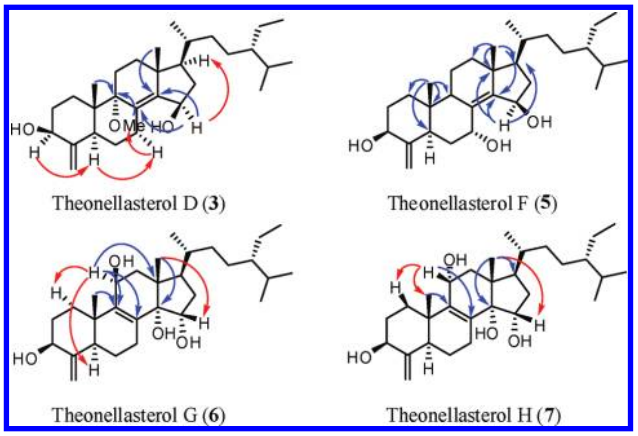

Figure 4. Key HMBC (blue arrows) and ROESY (red arrows) correlations for theonellasterols D (**3**), F (**5**), G (**6**), and H (**7**).

singlet Me-18 and a quaternary oxygenated carbon at δ_C 89.7 (Figure 4) allowed placement of a hydroxyl group at the C14 position, whereas the correlation between the Me-19 and the olefinic carbon at δ_C 142.5 evidenced the presence of a $\Delta^{8,9}$ double bond. Moreover, the localization of the secondary alcoholic function at C11 follows from the HMBC correlations between H-11 at δ_H 4.39 and C8, C9, and C13 (Figure 4), and a hydroxyl group was placed at C-15 by COSY analysis.

The relative configuration for the steroidal nucleus could be assigned by ROESY (Figure 4) and analysis of coupling constant data and on the basis of chemical shift considerations. The equatorial disposition of H-11 was evident from the small $^3J_{HH}$ vicinal coupling to H_2-12 and from the ROESY correlations to axial protons H-1 and H-5. The strong downfield shift exhibited by the H-17 was indicative of the α configuration of the 14 hydroxy group, whereas the α orientation of 15-OH was assigned on the basis of ROESY correlation between H-15 and Me-18 (Figure 4) and confirmed by ^{13}C chemical shift pattern of ring D nuclei.[15] Thus theonellasterol G (**6**) was defined as 4-methylene-24(*S*)-ethylcholest-8(9)-en-3β,11β,14α,15α-tetraol.

Theonellasterol H (**7**) showed the same molecular formula $C_{30}H_{50}O_4$ by HR ESIMS as **6**. Comparison of 1D NMR data of both compounds showed that they differed in ring C (Tables 1 and 2 and Tables S6 and S7 in Supporting Information). When compared with **6**, the chemical shifts of C9, C11, and C14 in theonellasterol H (**7**) were significatively upfield shifted, whereas those of C10, C12, and C13 were downfield shifted. These data suggested that the pseudoaxial 11-OH group in **6** has been replaced by a pseudoequatorial OH, as confirmed from ROESY correlations H-11/Me-19 and H-11/H-1β (Figure 4). As for **6**,

dx.doi.org/10.1021/jm200169t |J. Med. Chem. 2011, 54, 3065–3075

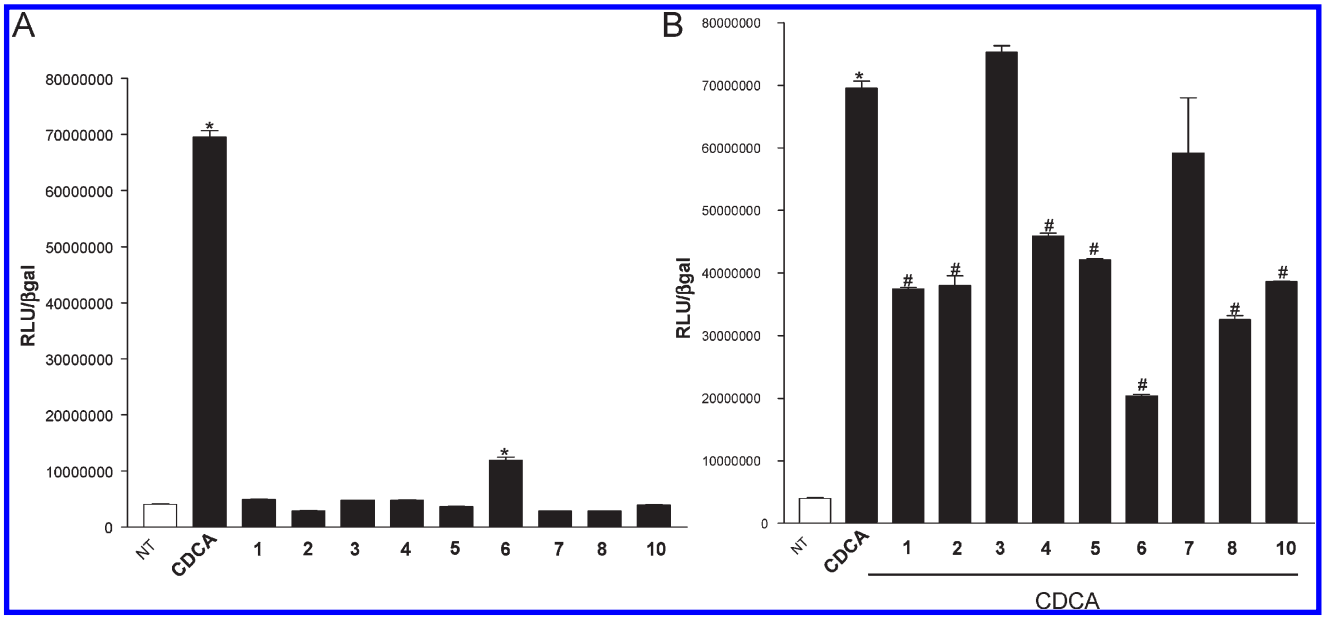

Figure 5. Luciferase reporter assay performed in HepG2 transiently transfected with pSG5-FXR, pSG5-RXR, pCMV-bgal, and p(hsp27)TKLUC vectors and stimulated 18 h with (A) CDCA, 10 μM, and compounds **1**−**8** and compound **10**, 10 μM. (B) CDCA, 10 μM, alone or in combination with compounds **1**−**8** and compound **10**, 50 μM. $^{*}P < 0.05$ versus not treated (NT). $^{\#}P < 0.05$ versus CDCA ($n = 4$).

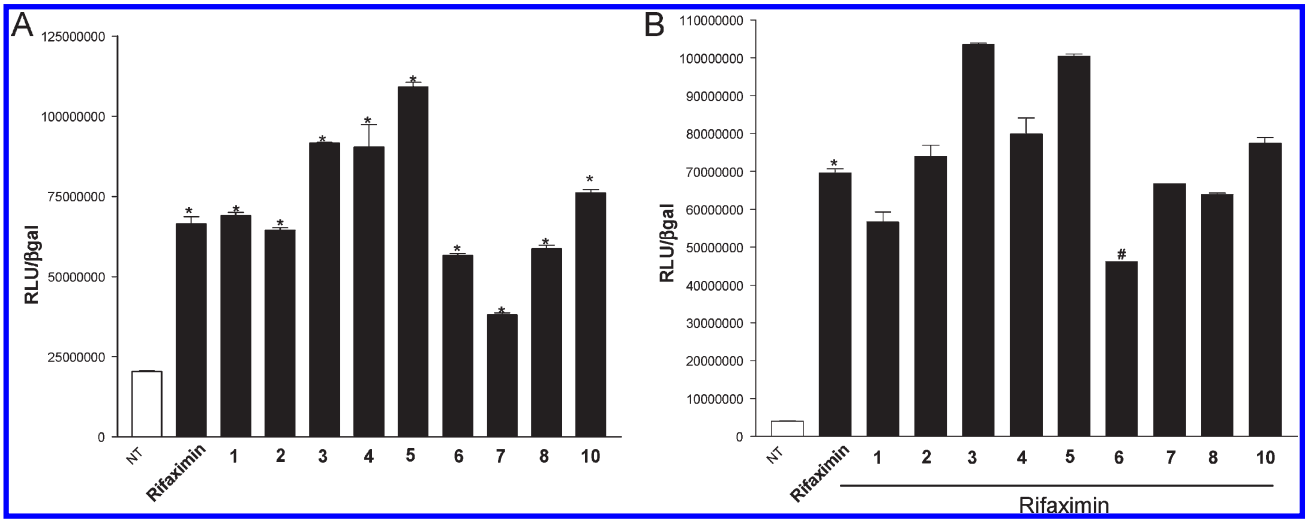

Figure 6. Luciferase reporter assay performed in HepG2 transiently transfected with pSG5-PXR, pSG5-RXR, pCMV-bgal, and p(cyp3a4)TKLUC vectors and stimulated 18 h with (A) rifaximin, 10 μM, and of compounds **1**−**8** and compound **10**, 10 μM. (B) Rifaximin, 10 μM, alone or in combination with compounds **1**−**8** and compound **10**, 50 μM. $^{*}P < 0.05$ versus not treated (NT). $^{\#}P < 0.05$ versus rifaximin ($n = 4$).

the α orientation of 15-OH and 14-OH was established by ROESY correlation H-15/Me-18 and on the basis of H-17 resonance, respectively. Therefore, theonellasterol H (**7**) was defined as 4-methylene-24(*S*)-ethylcholest-8(9)-en-3β,11α,14α,15α-tetraol.

Conicasterol B (**8**) was isolated as an optically active pale-yellow oil. The molecular formula of $C_{29}H_{44}O$, equivalent to theonellasterol B (**1**) less CH_2, was established by high resolution mass spectrometry. The ^{1}H and ^{13}C NMR spectra of **8** were very similar to **1** (Tables 1 and 2 and Table S1 in Supporting Information), with the steroid nucleus being identical. The only difference between compounds **1** and **8** appears to be in the steroidal side chain, with a methyl group at δ_H 0.85 (3H, d, $J = 7.0$ Hz) replacing the C24 ethyl group in **1**, thus accounting for the difference in molecular formula between the two molecules. The stereochemistry of the side chain was determined to be the same of conicasterol by comparison of $^{1}H^{16}$ and ^{13}C chemical shifts.[13]

Thus, conicasterol B (**8**) is 4-methylene-24(*R*)-methylcholest-7,9(11),14-trien-3β-ol.

Inspection of NMR data of conicasterols C (**9**) and D (**10**) (Tables 1 and 2) clearly evidenced a strong resemblance with theonellasterols D and E (Tables S3 and S4 in Supporting Information), respectively. Once again, the differences regarded the side chain with a methyl group (δ_H 0.88, 3H, d, $J = 6.7$ Hz in **9**; δ_H 0.89, 3H, d, $J = 6.8$ Hz in **10**) replacing the C24 ethyl group in compounds **3** and **4**. HRESIMS analysis gave definitively confirmation to the structures reported in Figure 3 as a 4-methylene-9α-methoxy-24(*R*)-methylcholest-8(14)-en-3β,15β-diol

dx.doi.org/10.1021/jm200169t |*J. Med. Chem.* 2011, 54, 3065–3075

for conicasterol C (**9**) and a 4-methylene-24(*R*)-methylcholest-8(14)-en-3β,9α,15β-triol for conicasterol D (**10**).

Biological Results. As a part of our continuing research directed toward the discovery of marine natural NRs ligands,[17] we recently demonstrated that the marine sponge *Theonella swinohei* produces steroids that act as NRs ligands. Solomonsterols A and B,[11] isolated from its polar extracts, are potent PXR agonists and new pharmacological anti-inflammatory leads. With this background in mind, we have investigated whether this family of hydroxylated sterols might act as modulators of two well characterized nuclear receptors, the farnesoid-X-receptor (FXR) and pregnane-X-receptor (PXR), highly expressed in the mammalian livers. For this purpose, compounds **1**−**8**[18] and compound **10** were challenged in a reporter gene assay using HepG2 cells, a human hepatoma cell line.

As illustrated in Figure 5A, all compounds, except theonellasterol G (**6**), that partially activated FXR, failed to activate FXR at the concentrations of 10 μM. By contrast, all compounds, with the exception of theonellasterols D (**3**) and H (**7**), effectively antagonized FXR transactivation induced by CDCA (Figure 5B). It is noteworthy that theonellasterol G (**6**) behaves as an antagonist in the presence of CDCA but is able to partially transactivate FXR, indicating that this agent is an FXR modulator. As shown in Figure 6A, at the concentration of 10 μM, all these compounds were PXR agonists. Interestingly, also theonellasterol G (**6**) acted as a PXR ligand, suggesting that this compound might be considered the first FXR modulator and PXR ligand so far identified. Indeed, when incubated with human hepatocytes, theonellasterol G (**6**) increased the expression of OSTα, a well-characterized FXR target (Figure 7B), along with SULT2A1 and MDR1, two well-characterized PXR responsive genes (Figure 7C and D). Thus, in agreement with transactivation experiments, the PCR data demonstrate that theonellasterol G (**6**) is an FXR modulator and PXR agonist.

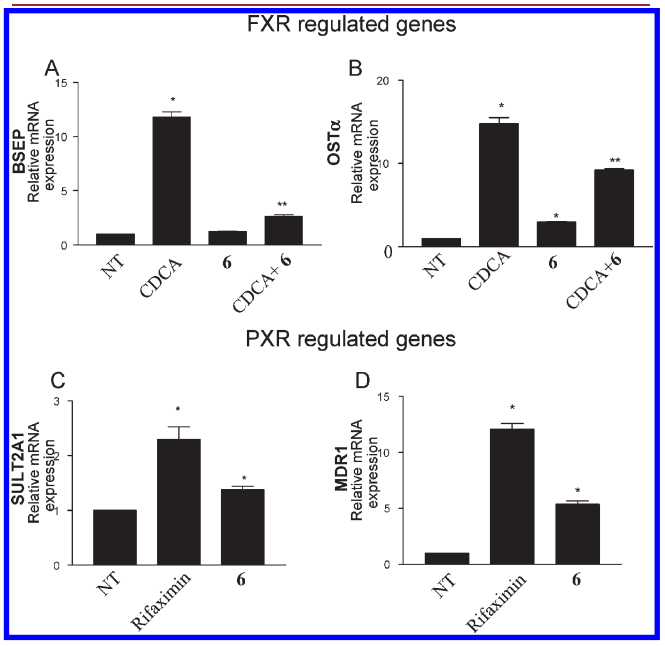

Figure 7. Real-time PCR analysis of (A) BSEP, (B) OSTα, (C) SULT2A1, and (D) MDR1 mRNAs expression carried out on cDNA isolated from HepG2 cells not treated (NT) or primed with 10 μM CDCA alone or in combination with 50 μM of **6** (A,B) or treated with rifaximin 10 μM (C,D). *P < 0.05 versus not treated. **P < 0.05 versus cells treated with CDCA.

Docking Studies. On the basis of the above-mentioned results, we have then analyzed, by means of molecular docking calculations, the interactions of polyhydroxylated steroids **1**−**8** and **10** with human FXR and PXR, in order to generate a structure−activity relationship and obtain information on their binding mode at atomic level. All the calculations were run by Autodock4.2 software.[19]

As shown in the Figure 8, compounds **1**−**8** and **10** adopt the same positioning in the FXR binding site when compared to 6-ECDCA. Even if the junction between A/B rings is *trans* and the OH group at position 3 is in the β position with respect to the cocrystallized molecule, for all the complex models relative to compounds **1**−**8** and **10**, the fundamental hydrogen bond contacts with the two amino acids of the catalytic triad[20] (namely Tyr358 in helix 7, His444 in helix 10/11) are maintained. Consequently, it is possible to single out two different docking poses for these molecules: (a) the first one regards compounds containing the OH group at position 3 and/or the OH group at position 15 in a *trans* relationship (**1**, **2**, **6**−**8**, Figure 8A), (b) the second family includes compounds having the 3- and 15- OHs in a relative *cis* arrangement (**3**−**5**, and **10**, Figure 8B). These results are also in agreement with the biological activity of our polyhydroxylated steroids (see above). Nevertheless, for all compounds **1**−**8** and **10**, the steroid nucleus is able to accommodate in the ligand binding site, establishing hydrophobic interactions with the cavity pocket formed between the Helix 2, 3, 5−7, and 10/11 (Figure 8).[20]

Concerning the interactions regarding other positions, the α-OH at position 9 of **4** and **10** forms a hydrogen bond with Ser329 (Helix 5) and this interaction is lost when the hydroxyl group is replaced by a methoxy group, as in compound **3**. Moreover, OH

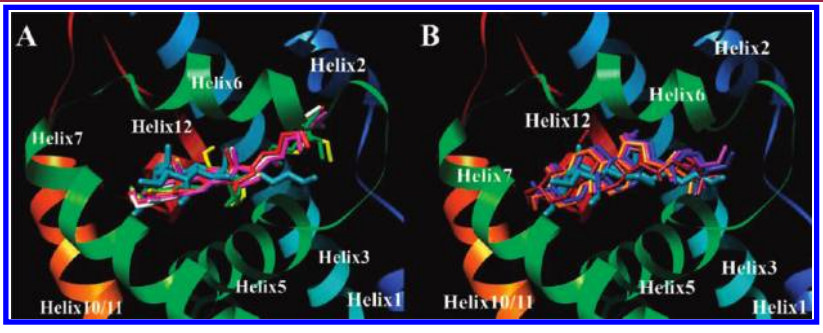

Figure 8. Two different spatial arrangements of polyhydroxylated steroids **1**−**8** and **10** in the binding site of FXR (chain A of crystal structure 1OSV). (A) Superposition of 6-ECDCA (light blue) with compounds **1** (pink), **2** (red), **6** (yellow), **7** (green), and **8** (white). (B) Superposition of 6-ECDCA (light blue) with compounds **3** (blue), **4** (purple), **5** (dark red), and **10** (orange).

dx.doi.org/10.1021/jm200169t |*J. Med. Chem.* 2011, 54, 3065–3075

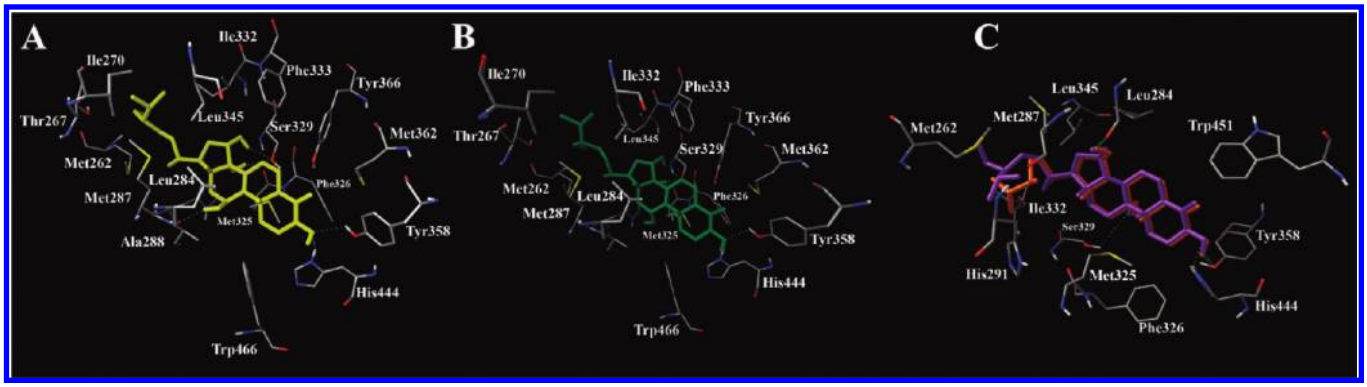

Figure 9. Three dimensional models of docking pose of **6** (A, yellow), **7** (B, green), **4** (C, purple) and **10** (**C**, orange) with FXR (see text for details).

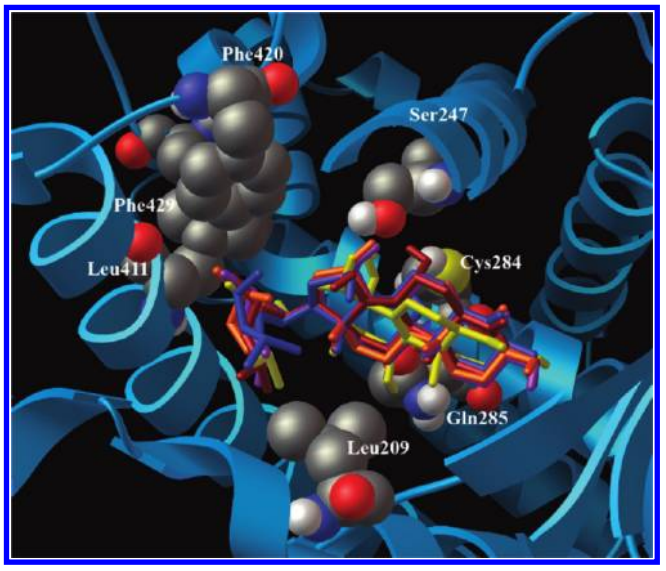

Figure 10. Three-dimensional model of the most representative polyhydroxylated steroids **3** (blue), **4** (purple), **5** (dark red), **6** (yellow), and **10** (orange) with the PXR binding pocket.

groups at 14α and 15α positions (compounds **6** and **7**, respectively) are able to establish hydrogen bonds with Ser329 (Helix 5), whereas the OH group at position 15β (compounds **3**−**5**, and **10**) interacts with Leu284 (Helix 3). The carbonyl group at position 15 (compound **2**) and the α-OH group at position 7 (compound **5**) do not exert further polar interactions with the FXR ligand binding site.

Regarding the side chain, the presence of a methyl group at position 24 for **8** and **10** allows stronger interactions with amino acids Met287 (Helix 3), Met262 (Coil 2), and His291 (Helix 3), present on the external part of the target molecular surface, with respect to compounds **1** and **4** bearing an ethyl group with different configuration (Figure 9C).

As previously reported,[21−24] the activation of FXR receptor by bile acids and bile acid analogues is affected by simultaneous presence of two α-OH at position 3 and 7 and by a good balance between hydrophobic and hydrophilic substituents at the α and β face of the nucleus. Moreover, Fujino et al.[21] have demonstrated that the introduction of β-alkyl and/or β-hydroxyl groups at 3 and/or 7 positions decreases the ligand potency.

This kind of interactions are missing for our compounds, and in fact all compounds, except theonellasterol G (**6**), failed in the activation of FXR at the concentration of 50 μM (see Biological Results section). In particular, as depicted in Figure 9A, the β-OH group at position 11 of compound **6** is involved in an additional hydrogen bond with Leu284 (Helix 3) with respect to its epimer **7** (Figure 9C), where this interaction is lost. Moreover, even if also **4** and **10** are able to interact with Ser329 (Helix 5) and Leu284 (Helix 3), they present a different spatial arrangement (Figures 8 and 9C) with respect to theonellasterol G (**6**), lacking some hydrophobic interactions with the amino acids of FXR ligand binding pocket (e.g., Trp466, Ile270, Thr267, Leu345, Figure 9). So, our docking calculations point out that the simultaneous interactions[25] of **6** with Helix 7 (Tyr358) and Helix 3 (Leu284) and its optimal hydrophobic contacts with the ligand binding domain compared to compounds **7** (only interacting with Helix 7) and **4** and **10**, respectively (Figures 7 and 8), cause a great difference in activity between these sterols, suggesting that a correct orientation of the OH group at position 11 and the hydrophobic contacts with the receptor are critical for the FXR modulator activity.

For what concerns the PXR[26] agonist activity, the first observation suggested by molecular docking analysis regards the positioning of compounds **1**−**8** and **10** in occupying in the region of PXR's expansive ligand binding pocket. As already reported,[26−30] this region is formed by hydrophobic (Phe251, Phe288, Phe429, Cys284, Leu206, Leu209, Leu324, Leu411, Met243, Met425, Trp299), polar, and charged (Ser247, Ser208, His407, Asp205, Arg410, Gln285) amino acids; particularly crucial is the interaction of our sterols with the Ser247, previously reported to be involved in key interactions for the PXR agonist activity.[17−21] In fact, this interaction is associated to the activity modulation observed in our series of compounds that is relative to substitution pattern of steroidal nucleus. It is noteworthy that 15α-OH, 15β-OH, and 15-keto substitutions are all possible H-bond acceptor sites interacting with H-bond donor Ser247. The further interactions of OH group at position 7 with Ser247 for compound **5**, of OH group at position 9 with Gln285 for **4**, and of OMe group at position 9 with Cys284 for **3**, may be responsible for the increased activity observed for these derivatives (Figure 10).

Finally, compounds **8** and **10**, featuring a methyl group at position 24, are endowed with a weaker agonist activity with respect to **1** and **4**, bearing an ethyl group with different configuration. Even though compounds **8** and **10** are able to interact by their side chain with Leu209, our models suggest that their decreased activity is due to lacking interactions with Phe420, Leu411, and Phe429 (Figure 10).

CONCLUSION

In summary, we have described a novel class of FXR/PXR modulators of marine origin.

Because PXR is a gene orchestrating the metabolism of xeno- and endobiotics by liver and intestinal epithelial cells[31] and, usually, PXR ligands are not ligand for FXR, the discovery of an ancestral dual activator highlights the potential for the existence of similar ligands in the mammalian body. From the pharmacology standpoint, a dual ligand holds potential in the treatment of liver disorders characterized by cholestasis and/or impaired metabolism of xenobiotics. Cholestasis is a liver disorder that occurs primarily in the context of genetic mutation of basolateral or apical transporters in hepatocytes and represents the main feature of primary biliary cirrhosis (PBC) and sclerosing cholangitis (PSC).[32−36] PBC and PSC are two immune-mediated disorders characterized by bile flow impairment due to progressive bile duct destruction for which medical therapy is still poorly effective. Treatment of PSC and PBC patients with agents that induce apical bile flow, however, is likely to fail to ameliorate the disease because the concomitant bile duct destruction. In contrast, animal studies have shown that agents that increase the basolateral flow, rather than hepatocyte's apical flow, might hold a strong therapeutic potential. Because BSEP is expressed at the apical pole of hepatocytes while OSTα is expressed at the basolateral membrane of hepatocytes, our results strongly support the testing of theonellasterol G (**6**) in a rodent model of cholestasis. Of relevance, because both FXR and PXR exert anti-inflammatory effects in the intestine, a dual ligand holds potential in the treatment of inflammatory bowel diseases. Moreover, docking analysis validated the experimental biological results and allowed rationalization of the peculiarity activity of theonellasterol G (**6**). The above results pave the way to design new selective and potent modulators for human nuclear receptors.

Finally, we have found that this series of marine sterols are endowed with potent PXR agonist activity and further studies are ongoing to define their potential applications in biomedical settings, such as liver toxicity induced by hepatotoxic drugs or sepsis.

All together, these results suggested that 4-methylene sterols, proposed as ideal taxonomic markers for Theonella sponges, are FXR antagonists and PXR agonists.

EXPERIMENTAL SECTION

General Procedures. Specific rotations were measured on a Perkin−Elmer 243 B polarimeter. High-resolution ESI-MS spectra were performed with a Micromass QTOF Micromass spectrometer. ESI-MS experiments were performed on an Applied Biosystem API 2000 triple-quadrupole mass spectrometer. NMR spectra were obtained on Varian Inova 500 and Varian Inova 700 NMR spectrometers (^{1}H at 500 and 700 MHz, ^{13}C at 125 and 175 MHz, respectively) equipped with a Sun hardware, δ (ppm), J in Hz, spectra referred to C_6HD_5 as internal standards (δ_H 7.16, δ_C 128.4). HPLC was performed using a Waters model 510 pump equipped with Waters Rheodine injector and a differential refractometer, model 401.

Through-space ^{1}H connectivities were evidenced using a ROESY experiment with mixing times of 200 and 500 ms, respectively.

Silica gel (200−400 mesh) from Macherey-Nagel Company was used for flash chromatography.

The purities of compounds were determined to be greater than 95% by HPLC.

Sponge Material and Separation of Individual Sterols. Two taxonomic vouchers (field collection references R3170 and R3144) both assigned to the widespread species *Theonella swinhoei* (order Lithistida, family Theonellidae) were collected on the barrier reef of Vangunu and Malaita Island, Solomon Islands, in July 2004. The samples were frozen immediately after collection and lyophilized to yield 600 and 355 g (dry mass) of R3170 and R3144, respectively. Taxonomic identification was performed by Dr. John Hooper of Queensland Museum, Brisbane, Australia, where specimens are deposited under the accession number G3122662 and G323969, respectively.

Theonella swinhoei (R3170). The lyophilized material (600 g) was extracted with methanol (3 × 2.7 L) at room temperature, and the methanolic extract, taken to dryness, was subjected to a modified Kupchan's partitioning procedure as follows. The methanol extract was dissolved in a mixture of MeOH/H_2O containing 10% H_2O and partitioned against *n*-hexane (19.7 g). The water content (% v/v) of the MeOH extract was adjusted to 30% and partitioned against $CHCl_3$ (17.8 g). The aqueous phase was concentrated to remove MeOH and then extracted with *n*-BuOH (10 g).

The hexane extract was chromatographed in two runs by silica gel MPLC using a solvent gradient system from CH_2Cl_2 to $CHCl_2$:MeOH 1:1.

Fractions eluted with CH_2Cl_2:MeOH 96:4 (419 mg) were further purified by HPLC on a Nucleodur 100−5 C18 (5 μm; 10 mm i.d. × 250 mm) with MeOH:H_2O (92:8) as eluent (flow rate 5 mL/min) to give 1.6 mg of theonellasterol H (**7**) (t_R = 9.5 min), 12 mg of theonellasterol G (**6**) (t_R = 11.6), 3.5 mg of theonellasterol F (**5**) (t_R = 12.4 min), 0.8 mg of conicasterol D (**10**) (t_R = 12.8 min), 3.3 mg of theonellasterol D (**3**) (t_R = 14.2 min), and 3.6 mg of theonellasterol E (**4**) (t_R = 16 min).

Fractions eluted with CH_2Cl_2:MeOH 95:5 (40 mg) were further purified by HPLC on a Nucleodur 100−5 C18 (5 μm; 10 mm i.d. × 250 mm) with MeOH:H_2O (92:8) as eluent (flow rate 5 mL/min) to give 0.6 mg of conicasterol B (**8**) (t_R = 7.8 min) and 0.8 mg of theonellasterol B (**1**) (t_R = 8.4 min).

Theonella swinhoei (R3144) was extracted with methanol (3 × 1.7 L) at room temperature, and the crude methanolic extract (32 g) was subjected to a modified Kupchan's partitioning procedure as described for *Theonella swinhoei* R3170 to obtain 3.9 g of *n*-hexane extract.

The hexane extract was chromatographed in two runs by silica gel MPLC using a solvent gradient system from CH_2Cl_2 to $CHCl_2$:MeOH 1:1.

Fractions eluted with CH_2Cl_2:MeOH 97:3 (15.5 mg) were further purified by HPLC on a Nucleodur 100−5 C18 (5 μm; 10 mm i.d. × 250 mm) with MeOH:H_2O (92:8) as eluent (flow rate 5 mL/min) to give 3.4 mg of theonellasterol D (**3**) and 1.1 mg of theonellasterol C (**2**) (t_R = 20.4 min). Fractions eluted with CH_2Cl_2:MeOH 94:6 (12.0 mg) were further purified by HPLC on a Nucleodur 100−5 C18 (5 μm; 10 mm i.d. × 250 mm) with MeOH:H_2O (92:8) as eluent (flow rate 5 mL/min) to give 1.2 mg of theonellasterol D (**3**), 4.0 mg of theonellasterol E (**4**), 0.5 mg conicasterol C (**9**) (t_R = 15 min), and 0.8 mg of conicasterol D (**10**).

Characteristic Data for Each Compound. *Theonellasterol B (**1**).* Pale yellow oil; $[\alpha]_D^{25}$ +1.6 (*c* 0.08, MeOH); UV (MeOH): λ_{max} (log ε) 275 nm (3.62); ^{1}H and ^{13}C NMR data in C_6D_6 given in Table S1 in Supporting Information; ESI-MS: m/z 429.4 $[M + Li]^+$. HRMS (ESI): calcd for $C_{30}H_{46}LiO$: 429.3709; found 429.3729 $[M + Li]^+$.

*Theonellasterol C (**2**).* Pale-yellow oil; $[\alpha]_D^{25}$ +5.7 (*c* 0.16, MeOH). ^{1}H and ^{13}C NMR data in C_6D_6 given in Table S2 in Supporting Information. ESI-MS: m/z 447.4 $[M + Li]^+$. HRMS (ESI): calcd for $C_{30}H_{48}LiO_2$ 447.3814; found 447.3834 $[M + Li]^+$.

*Theonellasterol D (**3**).* White amorphous solid; $[\alpha]_D^{25}$ +3.3 (*c* 0.17, MeOH). ^{1}H and ^{13}C NMR data in C_6D_6 given in Table S3 in Supporting Information. ESI-MS: m/z 479.4 $[M + Li]^+$. HRMS (ESI): calcd for $C_{31}H_{52}LiO_3$ 479.4076; found 479.4093 $[M + Li]^+$.

*Theonellasterol E (**4**).* White amorphous solid; $[\alpha]_D^{25}$ +34 (*c* 0.1, MeOH). ^{1}H and ^{13}C NMR data in C_6D_6 given in Table S4 in Supporting

Information. ESI-MS: m/z 465.4 $[M + Li]^+$. HRMS (ESI): calcd for $C_{30}H_{50}LiO_3$ 465.3920; found 465.3244 $[M + Li]^+$.

Theonellasterol F (**5**). White amorphous solid; $[\alpha]_D^{25}$ +4.3 (c 0.23, MeOH). ^1H and ^{13}C NMR data in C_6D_6 given in Table S5 in Supporting Information. ESI-MS: m/z 465.4 $[M + Li]^+$. HRMS (ESI): calcd for $C_{30}H_{50}LiO_3$ 465.3920; found 465.3247 $[M + Li]^+$.

Theonellasterol G (**6**). Pale-yellow oil; $[\alpha]_D^{25}$ +68 (c 1.0, MeOH). ^1H and ^{13}C NMR data in C_6D_6 given in Table S6 in Supporting Information. ESI-MS: m/z 481.4 $[M + Li]^+$. HRMS (ESI): calcd for $C_{30}H_{50}LiO_4$ 481.3869; found 481.3889 $[M + Li]^+$.

Theonellasterol H (**7**). Pale-yellow oil; $[\alpha]_D^{25}$ +16 (c 0.1, MeOH). ^1H and ^{13}C NMR data in C_6D_6 given in Table S7 in Supporting Information. ESI-MS: m/z 481.4 $[M + Li]^+$. HRMS (ESI): calcd for $C_{30}H_{50}LiO_4$ 481.3869; found 481.3875 $[M + Li]^+$.

Conicasterol B (**8**). Pale-yellow oil; $[\alpha]_D^{25}$ +29 (c 0.06, MeOH). UV (MeOH): λ_{max} (log ε) 275 nm (3.56). ^1H and ^{13}C NMR data in C_6D_6 given in Table S1 in Supporting Information. ESI-MS: m/z 415.4 $[M + Li]^+$. HRMS (ESI): calcd for $C_{29}H_{44}LiO$ 415.3552; found 415.3532 $[M + Li]^+$.

Conicasterol C (**9**). White amorphous solid; $[\alpha]_D^{25}$ +43 (c 0.13, MeOH). ^1H and ^{13}C NMR data in C_6D_6 given in Table S3 in Supporting Information. ESI-MS: m/z 465.4 $[M + Li]^+$. HRMS (ESI): calcd for $C_{30}H_{50}LiO_3$ 465.3920; found 465.3942 $[M + Li]^+$.

Conicasterol D (**10**). White amorphous solid; $[\alpha]_D^{25}$ +33 (c 0.08, MeOH). ^1H and ^{13}C NMR data in C_6D_6 given in Table S4 in Supporting Information. ESI-MS: m/z 451.4 $[M + Li]^+$. HRMS (ESI): calcd for $C_{29}H_{48}LiO_3$ 451.3763; found 451.3739 $[M + Li]^+$.

Plasmids, Cell Culture, Transfection, and Luciferase Assays. All transfections were made using Fugene HD transfection reagent (Roche). For FXR mediated transactivation, HepG2 cells, plated in a 6-well plate at 5×10^5 cells/well, were transfected with 100 ng of pSG5-FXR, 100 ng of pSG5-RXR, 200 ng of pCMV-βgalactosidase, and with 500 ng of the reporter vector p(hsp27)-TK-LUC containing the FXR response element IR1 cloned from the promoter of heat shock protein 27 (hsp27). At 48 h post-transfection, cells were stimulated 18 h with 10 μM CDCA or with the compounds **1**−**8** and **10** (10 μM) alone or in combination (50 μM) with CDCA.

For PXR mediated transactivation, HepG2 cells, plated in a 6-well plate at 5×10^5 cells/well, were transfected with 100 ng of pSG5-PXR, 100 ng of pSG5-RXR, 200 ng of pCMV-β-galactosidase, and with 500 ng of the reporter vector containing the PXR target gene promoter (CYP3A4 gene promoter) cloned upstream of the luciferase gene (pCYP3A4promoter-TKLuc). At 48 h post-transfection, cells were stimulated 18 h with 10 μM Rifaximin or with the compounds **1**−**8** and **10** (10 μM) alone or in combination with Rifaximin. Cells were lysed in 100 μL of diluted reporter lysis buffer (Promega) and 0.2 μL of cellular lysates was assayed for luciferase activity using the Luciferase Assay System (Promega). Luminescence was measured using an automated luminometer. Luciferase activities were normalized for transfection efficiencies by dividing the relative light units by β-galactosidase activity expressed from cells cotransfected with pCMV-βgal.

Quantitative Real-Time PCR. A 50 ng template was added to the PCR mixture (final volume 25 μL) containing the following reagents: 0.2 μM of each primer and 12.5 μL of 2X SYBR Green qPCR master mix (Invitrogen, Milan, Italy). All reactions were performed in triplicate, and the thermal cycling conditions were: 2 min at 95 °C, followed by 40 cycles of 95 °C for 20 s, 55 °C for 20 s, and 72 °C for 30 s in iCycler iQ instrument (Biorad, Hercules, CA). The mean value of the replicates for each sample was calculated and expressed as cycle threshold (C_T: cycle number at which each PCR reaction reaches a predetermined fluorescence threshold, set within the linear range of all reactions). The amount of gene expression was then calculated as the difference (ΔC_T) between the C_T value of the sample for the target gene and the mean C_T value of that sample for the endogenous control (GAPDH). Relative expression was calculated as the difference ($\Delta\Delta C_T$) between the ΔC_T values of the test sample and of the control sample (not treated) for each target gene. The relative quantitation value was expressed and shown as $2^{-\Delta\Delta C_T}$. All PCR primers were designed with PRIMER3-OUTPUT software using published sequence data from the NCBI database. The primers sequence were as follows: hBSEP: gggccattgtacgagatcctaa and tgcaccgtcttttcactttctg; hOSTα: tgttgggccctttccaatac and ggctcccatgttctgctcac; hGAPDH: gaaggtgaaggtcggagt and catgggtggaatcatattggaa; hSULT2A1: gatccaatctgtgcccatct and taaatcaccttggccttgga; hMDR1: gtggggcaagtcagttcatt and tcttcacctccaggctcagt.

Computational Details. Molecular docking calculations were performed by Autodock4.2 software on quad-core Intel Xeon 3.4 GHz. A grid box size of 94 × 96 × 68 for FXR receptor, and of 90 × 106 × 92 for PXR rceptor with spacing of 0.375 Å between the grid points and centered for FXR at 20.689 (x), 39.478 (y), and 10.921 (z), and for PXR at 14.282 (x), 74.983 (y), and 0.974 (z) covering the active site on the two targets surface was used. The Lamarckian genetic algorithm with an initial population of 600 randomly placed individuals, a maximum number of 5.0×10^6 energy evaluations, and a maximum number of 6.0×10^6 generations were taken into account for dockings by Autodock4.2 software. A mutation rate of 0.02 and a crossover rate of 0.8 were used. Results differing by less than 3.5 Å in positional root-mean-square deviation (rmsd) were clustered together and represented by the result with the most favorable free energy of binding. Illustrations of the 3D models were generated using the Chimera[37] and the Python software.[38]

■ ASSOCIATED CONTENT

Supporting Information. One- and two-dimensional NMR spectra and tabulated NMR data of compounds **1**−**10**. This material is available free of charge via the Internet at http://pubs.acs.org.

■ AUTHOR INFORMATION

Corresponding Author

*Phone: (0039) 081-678525. Fax (0039) 081-678552. E-mail: angela.zampella@unina.it.

Author Contributions

⊥Contributed equally to this work.

■ ACKNOWLEDGMENT

NMR spectra were provided by the CSIAS, Centro Interdipartimentale di Analisi Strumentale, Faculty of Pharmacy, University of Naples. We thank the Solomon Islands government for collection permits, the Fisheries Department, and R. Sulu (University of the South Pacific in Honiara) for their help and assistance and Dr. John Hooper for the identification of the sponges.

■ ABBREVIATIONS USED

BAs, bile acids; BSEP, bile salt export pump; CDCA, chenodeoxycholic acid; COSY, correlation spectroscopy; FXR, farnesoid-X-receptor; HepG2, human hepatoma cell line; HR ESIMS, high-resolution electrospray ionization mass spectrometry; HMBC, heteromultibond correlation; HSQC, heteronuclear single-quantum coherence; MDR1, multidrug resistance 1; NRs, nuclear receptors; OSTα, organic solute transporter alpha; PBC, primary biliary cirrhosis; PDB, Protein Data Bank; PSC, primary sclerosing cholangitis; PXR, pregnane-X-receptor; ROESY,

rotating frame nuclear Overhauser effect spectroscopy; RT PCR, real-time polymerase chain reaction; SULT2A1, sulfotransferase 2A1

REFERENCES

(1) Zhang, H. J.; Yi, Y. H.; Lin, H. W. Oxygenated 4-methylidene sterols from the South China Sea sponge *Theonella swinhoei*. *Helv. Chim. Acta* **2010**, *93*, 1120–1126.

(2) Kho, E.; Imagawa, D. K.; Rohmer, M.; Kashman, Y.; Djerassi, C. Sterols in marine invertebrates. 22. Isolation and structure elucidation of conicasterol and theonellasterol, two new 4-methylene sterols from the Red Sea sponges *Theonella conica* and *Theonella swinhoei*. *J. Org. Chem.* **1981**, *46*, 1836–1839.

(3) Angawi, R. F.; Calcinai, B.; Cerrano, C.; Dien, H. A.; Fattorusso, E.; Scala, F.; Taglialatela-Scafati, O. Dehydroconicasterol and aurantoic acid, a chlorinated polyene derivative, from the indonesian sponge *Theonella swinhoei*. *J. Nat. Prod.* **2009**, *72*, 2195–2198.

(4) Kobayashi, M.; Kawazoe, K.; Katori, T.; Kitagawa, I. Marine Natural Products. XXX. Two new 3-keto-4-methylene steroids, theonellasterone and conicasterone, and a Diels−Alder type dimeric steroid bistheonellasterone, from the Okinawan marine sponge *Theonella swinhoei*. *Chem. Pharm. Bull.* **1992**, *40*, 1773–1778.

(5) Qureshi, A.; Faulkner, D. J. 7α-Hydroxytheonellasterol, a cytotoxic 4-methylene sterol from the philippines sponge *Theonella swinhoei*. *J. Nat. Prod.* **2000**, *63*, 841–842.

(6) Sugo, Y.; Inouye, Y.; Nakayama, N. Structures of nine oxygenated 4-methylene sterols from Hachijo marine sponge *Theonella swinhoei*. *Steroids* **1995**, *60*, 738–742.

(7) Coral Reef Initiative in The South Pacific (CRISP).

(8) Festa, C.; De Marino, S.; Sepe, V.; Monti, M. C.; Luciano, P.; D'Auria, M. V.; Debitus, C.; Bucci, M.; Vellecco, V.; Zampella, A. Perthamides C and D, two new potent anti-inflammatory cyclopeptides from a Solomon Lithistid sponge *Theonella swinhoei*. *Tetrahedron* **2009**, *65*, 10424–10429.

(9) Sepe, V.; D'Auria, M. V; Bifulco, G.; Ummarino, R.; Zampella, A. Concise synthesis of AHMHA unit in perthamide C. Structural and stereochemical revision of perthamide C. *Tetrahedron* **2010**, *66*, 7520–7526.

(10) Festa, C.; De Marino, S.; Sepe, V.; D'Auria, M. V.; Bifulco, G.; Debitus, C.; Bucci, M.; Vellecco, V.; Zampella, A. Solomonamides A and B, new anti-inflammatory peptides from *Theonella swinhoei*. *Org. Lett.* **2011**, *13*, 1532–1535.

(11) Festa, C.; De Marino, S.; D'Auria, M. V.; Bifulco, G.; Renga, B.; Fiorucci, S.; Petek, S.; Zampella, A. Solomonsterols A and B from *Theonella swinhoei*. The first example of C-24 and C-23 sulfated sterols from a marine source endowed with a PXR agonistic activity. *J. Med. Chem.* **2011**, *54*, 401–405.

(12) All steroids in the present study showed a more or less chemical instability when $CDCl_3$ solutions were left standing; therefore we used C_6D_6 as solvent for NMR experiments.

(13) Wright, J. L. C.; Mclnnes, A. G.; Shimizu, S.; Smith, D. G.; Walter, J. A.; Idler, D.; Khalil, W. Identification of C-24 alkyl epimers of marine sterols by carbon-13 nuclear magnetic resonance spectroscopy. *Can. J. Chem.* **1978**, *56*, 1898–1903.

(14) Horibe, I.; Nakai, H.; Sato, T.; Seo, S.; Takeda, K.; Takatsuto, S. Stereoselective synthesis of the C-24 and C-25 stereoisomeric pairs of 24-ethyl-26-hydroxy- and 24-ethyl-[26-2*H*]sterols and their Δ22-derivatives: reassignment of ^{13}C NMR signals of the pro-*R* and the pro-*S* methyl groups at C-25 of 24-ethylsterols. *J. Chem. Soc., Perkin Trans. 1* **1989**, 1957–1967.

(15) Wang, F.; Fang, Y.; Zhang, M.; Lin, A.; Zhu, T.; Gu, Q.; Zhu, W. Six new ergosterols from the marine-derived fungus *Rhizopus* sp. *Steroids* **2008**, *73*, 19–26.

(16) Rubinstein, I.; Goad, L. J.; Clague, A. D. H.; Mulheirn, L. J. The 220 MHz NMR spectra of phytosterols. *Phytochemistry* **1976**, *15*, 195–200.

(17) Sepe, V.; Bifulco, G.; Renga, B.; D'Amore, C.; Fiorucci, S.; Zampella, A. Discovery of sulfated sterols from marine invertebrates as a new class of marine natural antagonists of farnesoid-X-receptor. *J. Med. Chem.* **2011**, *54*, 1314–1320.

(18) Isolation of conicasterol C (**9**) in very small amounts hampered its pharmacological evaluation.

(19) Morris, G. M.; Huey, R.; Lindstrom, W.; Sanner, M. F.; Belew, R. K.; Goodsell, D. S.; Olson, A. J. AutoDock4 and AutoDockTools4: automated docking with selective receptor flexibility. *J. Comput. Chem.* **2009**, *30*, 2785–2791.

(20) Mi, L. -Z.; Devarakonda, S.; Harp, J. M.; Han, Q.; Pellicciari, R.; Willson, T. M.; Khorasanizadeh, S.; Rastinejad, F. Structural basis for bile acid binding and activation of the nuclear receptor FXR. *Mol. Cell* **2003**, *11*, 1093–1100.

(21) Fujino, T.; Une, M.; Imanaka, T.; Inoue, K.; Nishimaki-Mogami, T. Structure−activity relationship of bile acids and bile acid analogs in regard to FXR activation. *J. Lipids Res.* **2004**, *45*, 132–138.

(22) Modica, S.; Gadaleta, R. M; Moschetta, A. Deciphering the nuclear bile acid receptor FXR paradigm. *Nucl. Recept. Signaling* **2010**, *8*, 1–28.

(23) Downes, M.; Verdecia, M. A.; Roecker, A. J.; Hughes, R.; Hogenesch, J. B.; Kast-Woelbern, H. R.; Bowman, M. E.; Ferrer, J. −L.; Anisfeld, A. M.; Edwards, P. A.; Rosenfeld, J. M.; Alvarez, J. G. A.; Noel, J. P.; Nicolaou, K. C; Evans, R. M. A Chemical, genetic, and structural analysis of the nuclear bile acid receptor FXR. *Mol. Cell* **2003**, *11*, 1079–1092.

(24) Wang, H.; Chen, J.; Hollister, K.; Sowers, L. C.; Forman, B. M. Endogenous bile acids are ligands for the nuclear receptor FXR/BAR. *Mol. Cell* **1999**, *3*, 543–553.

(25) Kuipers, F.; Claudel, T.; Sturm, E.; Staels, B. The farnesoid X receptor (FXR) as modulator of bile acid metabolism. *Rev. Endocr. Metab. Disord.* **2004**, *5*, 319–326.

(26) Watkins, R. E.; Maglich, J. M.; Moore, L. B.; Wisely, G. B.; Noble, S. M.; Davis-Searles, P. R.; Lambert, M. H.; Kliewer, S. A.; Redinbo., M. R. 2.1 Å Crystal structure of human PXR in complex with the St. John's Wort compound hyperforin. *Biochemistry* **2003**, *42*, 1430–1438.

(27) Ekins, S.; Chang, C.; Mani, S.; Krasowski, M. D.; Reschly, E. J.; Iyer, M.; Kholodovych, V.; Ai, N.; Welsh, W. J.; Sinz, M.; Swaan, P. W.; Patel, R.; Bachmann, K. Human Pregnane X receptor antagonists and agonists define molecular requirements for different binding sites. *Mol. Pharmacol.* **2007**, *72*, 592–603.

(28) Watkins, R. E.; Wisely, G. B.; Moore, L. B.; Collins, J. L.; Lambert, M. H.; Williams, S. P.; Willson, T. M.; Kliewer, S. A.; Redinbo., M. R. The human nuclear xenobiotic receptor PXR: structural determinants of directed promiscuity. *Science* **2001**, *292*, 2329–2333.

(29) Ekins, S.; Kortagere, S.; Iyer, M.; Reschly, E. J.; Lill, M. A.; Redinbo, M. R.; Krasowski, M. D. Challenges predicting ligand receptor interactions of promiscuous proteins: the nuclear receptor PXR. *PLoS Comput. Biol.* **2009**, *5*, e1000594.

(30) Xue, Y.; Moore, L. B.; Orans, J.; Peng, L.; Bencharit, S.; Kliewer, S. A.; Redinbo, M. R. Crystal structure of the pregnane X receptor-estradiol complex provides insights into endobiotic recognition. *Mol. Endocrinol.* **2007**, *21*, 1028–1038.

(31) Rock, K. L.; Latz, E.; Ontiveros, F.; Kono, H. The sterile inflammatory response. *Annu. Rev. Immunol.* **2010**, *28*, 321–342.

(32) Fiorucci, S.; Mencarelli, A.; Palladino, G.; Cipriani, S. Bile-acid-activated receptors: targeting TGR5 and farnesoid-X-receptor in lipid and glucose disorders. *Trends Pharmacol. Sci.* **2009**, *30*, 570–580.

(33) Fiorucci, S.; Baldelli, F. Farnesoid X receptor agonists in biliary tract disease. *Curr. Opin. Gastroenterol.* **2009**, *25*, 252–259.

(34) Fiorucci, S.; Cipriani, S.; Mencarelli, A.; Renga, B.; Distrutti, E.; Baldelli, F. Counter-regulatory role of bile acid activated receptors in immunity and inflammation. *Curr. Mol. Med.* **2010**, *10*, 579–595.

(35) Fiorucci, S.; Mencarelli, A.; Distrutti, E.; Palladino, G.; Cipriani, S. Targeting farnesoid-X-receptor: from medicinal chemistry to disease treatment. *Curr. Med. Chem.* **2010**, *17*, 139–159.

(36) Fiorucci, S.; Cipriani, S.; Baldelli, F.; Mencarelli, A. Bile acid-activated receptors in the treatment of dyslipidemia and related disorders. *Prog. Lipid Res.* **2010**, *49*, 171–185.

(37) Pettersen, E. F.; Goddard, T. D.; Huang, C. C.; Couch, G. S.; Greenblatt, D. M.; Meng, E. C.; Ferrin, T. E. UCSF Chimera? A visualization system for exploratory research and analysis. *J. Comput. Chem.* **2004**, *25*, 1605–1612.

(38) Sanner, M. F. Python: A Programming Language for Software Integration and Development. *J. Mol. Graphics Modell.* **1999**, *17*, 57–61.